Research Paper

Exploration of cuprotosis-related genes for predicting prognosis and immunological characteristics in acute myeloid leukaemia based on genome and transcriptome

Yanhui Wei[1,2], Zhaoxu Miao[2], Xuejun Guo[2,3], Songwei Feng[4,&]

[1]School of Medicine, Southeast University, Nanjing, China
[2]Department of Haematology, Puyang Oilfield General Hospital, Puyang, China
[3]Puyang Translational Medicine Engineering and Technology Research Center, Puyang, China
[4]Department of Obstetrics and Gynaecology, Zhongda Hospital, School of Medicine, Southeast University, Nanjing, China

Correspondence to: Xuejun Guo, Songwei Feng; **email:** pygxj@163.com, https://orcid.org/0000-0002-9840-9378; soochowfengsw@163.com, https://orcid.org/0009-0003-5519-3663

ABSTRACT

Background: Acute myeloid leukemia (AML) is a common hematologic malignancy with a generally unfavorable prognosis. Cuprotosis as a new form of programmed cell death has been shown to play an important role in tumorigenesis and progression; However, the relationship between cuprotosis and the prognosis of AML patients remains unclear.
Methods: Transcriptomic and genomics data, along with clinical information, were obtained from the TCGA and GEO databases. Especially, unsupervised clustering and machining learning were used to identify molecular subtypes and cuprotosis-related risk scores respectively. Kaplan-Meier analysis, univariate and multivariate Cox regression, and Receiver Operator Characteristic curve (ROC) were performed to assess the prognosis based on cuprotosis-related genes (CRGs). Moreover, multiple algorithms were used to evaluate immunological heterogeneity among patients with different risk scores. For *in vitro* analysis, the expression of genes involved in CRGs was detected by Quantitative Reverse Transcription Polymerase (qRT-PCR) in AML patients.
Results: Transcriptomic and genome data indicated the immense heterogeneity in the CRGs landscape of normal and tumor samples. Cuprotosis subtype A and cuprotosis regulatory subtype B in the genomics map and biological characteristics were significantly different from the other groups. Furthermore, these two subtypes had lower risk scores and longer survival times compared to other groups. Cox analyses indicated that risk score was an independent prognostic factor for AML patients. In addition, our risk score could be an indicator of survival outcomes in immunotherapy datasets.
Conclusions: Our study demonstrates the potential of CRGs in guiding the prognosis, treatment, and immunological characteristics of AML patients.

INTRODUCTION

Acute myeloid leukemia (AML) is a cancerous condition that affects the hematopoietic system and is characterized by abnormal proliferation, hindered differentiation, and diminished apoptosis of stem cells [1–4]. The pathogenesis of AML is rooted in molecular genetics and cytogenetic alterations, which also have an

impact on the prognosis and treatment of the disease [5, 6]. Despite recent advancements in immunotherapy, there are notable variations in the prognosis of individual patients, and current prognostic classification systems appear inadequate in providing precise assessments for diverse individuals [7]. Consequently, it is imperative to identify new biomarkers that can accurately predict patient prognosis.

Programmed cell death (PCD) is a natural biological process that plays a crucial role in maintaining the stability of an organism. There are several recognized forms of cell death, including apoptosis, pyroptosis, necrosis, ferroptosis, and cuprotosis [8, 9]. Cuprotosis is another way of PCD induced by metal ions after ferroptosis, discovered by Tsvetkov and his colleagues in 2022 [10]. As a cofactor for essential enzymes, copper ions maintain a low concentration and maintain a dynamic balance [11], and play an important role in the homeostasis of cells, the accumulation and imbalance of intracellular copper ions will be toxic to cells and even induce cell death [12]. The study found that cuprotosis is caused by an excess of intracellular copper transported to mitochondria via ion carriers and directly bound to lipid-acylated components of the tricarboxylic acid cycle during mitochondrial respiration, resulting in the aggregation of lipid-acylated proteins and loss of iron-sulfur cluster proteins, which induces proteotoxic stress and ultimately leads to cell death [10, 13]. Cuprotosis, as a newly discovered form of PCD, holds potential in the diagnosis and treatment of tumors [14], however, the relationship between cuprotosis-related genes and AML (non-M3) prognosis is unclear and is an area of ongoing research.

In this study, we downloaded gene expression data from The Cancer Genome Atlas (TCGA) database for the AML cohort and matched clinical data, and we determined the prognostic value of CRGs for AML. In addition, we also delved into the impact of CRGs on the immune microenvironment of AML patients. Our findings indicate that the CRGs have the potential to provide an effective and precise prediction of the prognosis for AML patients. Importantly, these findings also offer novel insights into the immunotherapy of AML.

MATERIALS AND METHODS

Data collection

The TCGA-LAML dataset was downloaded from the TGCA database, and GSE37642 (GSE37642-GPL96, GSE37642-GPL570) and GSE12417 (GSE12417-GPL96, and GSE12417-GPL570) were downloaded from the GEO database. Mutation data and copy number variation (CNV) data were also downloaded from TCGA database. We used the "sva" package to eliminate the batch effect in RNA-seq and microarray, Finally, we annotated 11,1917 protein-coding mRNA in the meta dataset. We excluded incomplete survival information, non-whole bone marrow sequencing, M3, and repeated sequencing samples. Finally, 116 patients were included in the TCGA cohort, 539 patients in the GSE37642 cohort, and 233 patients in the GSE12417 cohort. Cuprotosis-related genes (CRGs) were collected from previous references. The expression data were log2 transformed and normalized. The Gene MANIA database was used to construct protein-protein interactions (PPI) network.

Unsupervised consensus clustering

In the meta-cohort (combined TCGA dataset and GEO dataset), based on prognostic CRGs, we used unsupervised consistent clustering ("ConsensusClusterPlus" package) to divide all patients and principal component analysis (PCA) was used to determine whether each subtype was relatively independent of the others. Importantly, 1000 repetitions were performed, pItem = 0.8, to verify the stability of the subtype in unsupervised consistent clustering.

Functional enrichment analysis

Gene set variation analysis (GSVA) was used to evaluate differences in biological pathways between subtypes, using c2.cp.kegg.v7.0.symbol as a reference gene set, FDR < 0.05 was the threshold. Moreover, we used the "limma" package to analyze the differential expression genes (DEGs) between different subtypes, next, we used "clusterProfiler" package for functional enrichment based on DEGs, *P*-value < 0.05 and *q*-value < 0.05 was the threshold.

Tumor immune microenvironment

Overall, following the pipeline in previous studies, we used eight algorithms (TIMER, CIBERSORT, QUANTISEQ, MCP-counter, XCELL, EPIC, ssGSEA, and ESTIMATE) to estimate the abundances of immune cells for each sample in TCGA and GEO dataset.

Response to targeted drugs

Relevant references have confirmed the important role of the cell cycle, PI3K/mTOR pathway, and Wnt pathway in the progression of AML. Hence, we used the "pRRophetic" package to calculate the half maximal inhibitory concentration (IC50) of different targeted drugs, including CGP.60474 (cell cycle), JW.7.52.1 (PI3K/mTOR), and CHIR.99021 (Wnt).

Table 1. Primer sequences.

Gene	Primer sequences (5′–3′)
β-actin-F	CACCCTGAAGTACCCCATCG
β-actin-R	GATAGCACAGCCTGGATAGCA
LIPT1-F	TGGATGTGCAGGCTACCAAA
LIPT1-R	CGGCCGATCTTAGAAGCTGT
DBT-F	ACCTGAAGTAGCCATTGGGG
DBT-R	AGCGTGACATTGTAGCACCA
DLST-F	CTGCCTGGGGTCTCCTTATG
DLST-R	AAACGCTGGGGTTTTGACTG

Machine learning-derived risk cuprotosis-related risk score

We performed our previous workflow to construct a consensus prognosis model for AML patients. Firstly, we constructed 55 combination of machine learning algorithms based on nine algorithms, including LASSO, GBM, Survival-SVM, SuperPC, ridge regression, plsRcox, CoxBoost, StepCox, and Enet [15]. We used models that can perform variable filtering as the pre-model. Subsequently, we used the GSE37642 as the training set to construct signatures in prognostic DEGs matrix based on different cuprotosis subtypes. We selected the best consensus prognostic model based on the mean C-index of the three cohorts (GSE37642, TCGA-LAML and GSE12417). Risk score was calculated for each patient based on the expression of each candidate variable and the coefficients in the final model. ROC curve was used to evaluate the predictive performance of risk score for OS. The prognostic difference was analyzed by Kaplan-Meier analysis and log-rank test. In addition, we downloaded the IMvigor-210 cohort, and GSE78220 cohort from the previous references to generate a risk score and verify the effect of the risk score in the immunotherapy cohort.

Quantitative real-time polymerase chain reaction

Peripheral blood samples were collected from AML patients (12 cases) and healthy volunteers (11 cases) from Puyang Oilfield General Hospital. Patient RNA was extracted by Trizol reagent (Invitrogen, Carlsbad, CA, USA) according to the manufacturer's protocol and cDNA was synthesized by reverse transcription kits (TAKARA, Japan). QRT-PCR was performed using a Step One Plus qRT-PCR machine (Applied Biosystems, Waltham MA, USA). All primers were provided by Suzhou Jinweizhi Biotechnology Co., Ltd (Jiangsu, China). The primer sequences as shown in Table 1.

Statistical analysis and software

The statistical analyses were conducted in the R software (version 4.1.2). Specific statistical methods have been mentioned in the bioinformatics methods above. [***], [**], [*], ns refers to $p < 0.001$, < 0.01, < 0.05, and not significant, respectively. The Microsoft Office PowerPoint software is used to generate images for this article.

RESULTS

Genetic variation and expression of cuprotosis-related regulatory genes in AML

We first explored the landscape of 12 annotated CRGs in meta cohorts. The location of the 12 CRGs in the chromosomes was shown (Figure 1A). We further compared the expression of these 12 CRGs in different risk categories (ELN 2017 risk category) of AML. Among AML patients in different risk categories, we found differences in DLD, LIAS, FDX1, ATP7A, and PDHD in the ELN 2017 risk category (Figure 1B). Furthermore, we compared the expression of 12 CRGs between normal and AML samples, and the results showed the expression of 11 CRGs (except for PDHB) was significantly different in normal and AML patients (Figure 1C, 1D). In detail, the expression of genes LIPT1, DBT, and DLST were significantly higher in AML patients. We also found CNV amplification in FDX1, DLAT, ATP7B, DBT, DLST and LIPT1 among these 12 CRGs, while mainly showed loss in other CRGs (Figure 1E). We also found DLD mutations with a frequency of only 1% (Figure 1F). The above results showed the expression difference maybe not be caused by somatic mutations, but by CNV.

Analysis of the characteristics of different cuprotosis subtypes

We investigated the relationships between the 12 CRGs, and the network showed that all 12 CRGs were associated (Figure 2A). Multiple data sets were normalized to increase the sample size (Supplementary Figure 1). In the network of survival and correlation analysis, the results showed that 12 CRGs were still highly associated (Figure 2B). In addition, we investigated the prognostic value of 12 CRGs, we carried out Kaplan-Meier analysis of each CRGs, and

the results showed that 11 CRGs had statistical significance on the overall survival (Supplementary Figure 2). Then, we divided AML patients into 3 subtypes, called cuprotosis subtypes A (n = 158), B (n = 426), and C (n = 304) (Figure 2C). The above various subtypes were demonstrated by PCA to be independent of one another over the whole gene expression spectrum (Figure 2D). Patients with subtype A had the best
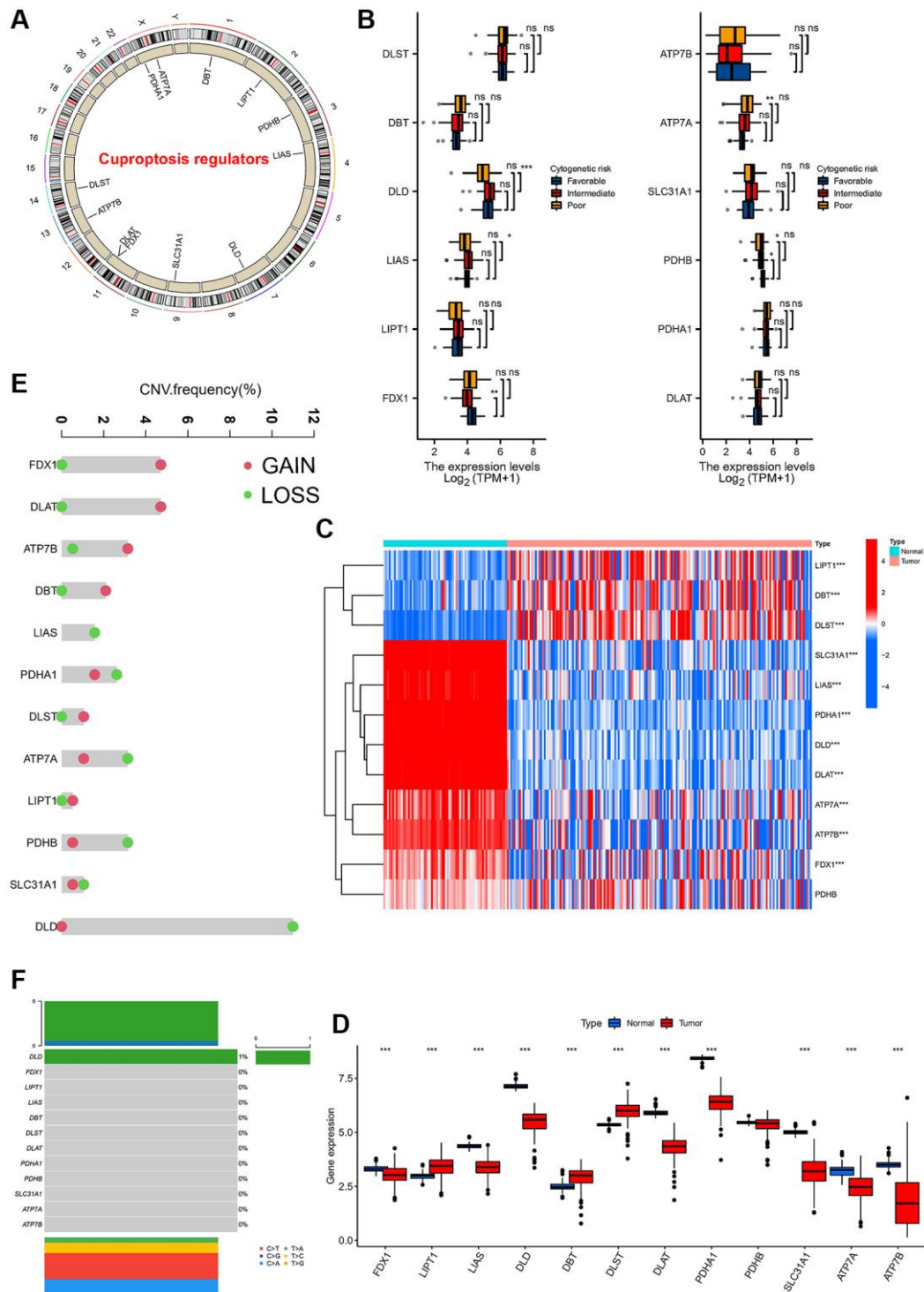

Figure 1. Expression and variation profiles of 12 cuprotosis-related genes in AML patients. (**A**) Location of CNV of 12 Cuprotosis genes on chromosomes. (**B**) Expression of 12 cuprotosis-related genes in AML patients with different risk stratification. (**C**) Heat map of cuprotosis-related genes in AML patients and normal population. (**D**) Difference in the expression level of cuprotosis-related genes between normal and tumour samples. (**E**) CNV frequency of Cuprotosis genes, the copy number amplification, green dot; the copy number deletion, red dot. (**F**) Mutation frequency of 12 cuprotosis-related genes in 130 samples. (*$P < 0.05$, **$P < 0.01$, ***$P < 0.001$).

survival compared to other subtypes, according to a Kaplan-Meier analysis (Figure 2E). We further analyzed the expression of 12 CRGs in the three subtypes and all 12 CRGs were significantly differentially expressed in three cuprotosis subtypes (Figure 2F).

To investigate the immunological characteristics of the three cuprotosis subtypes, we analyzed the relationship between the aforementioned cuprotosis subtypes and immune cells. The results revealed significant differences among the three subtypes in the level of
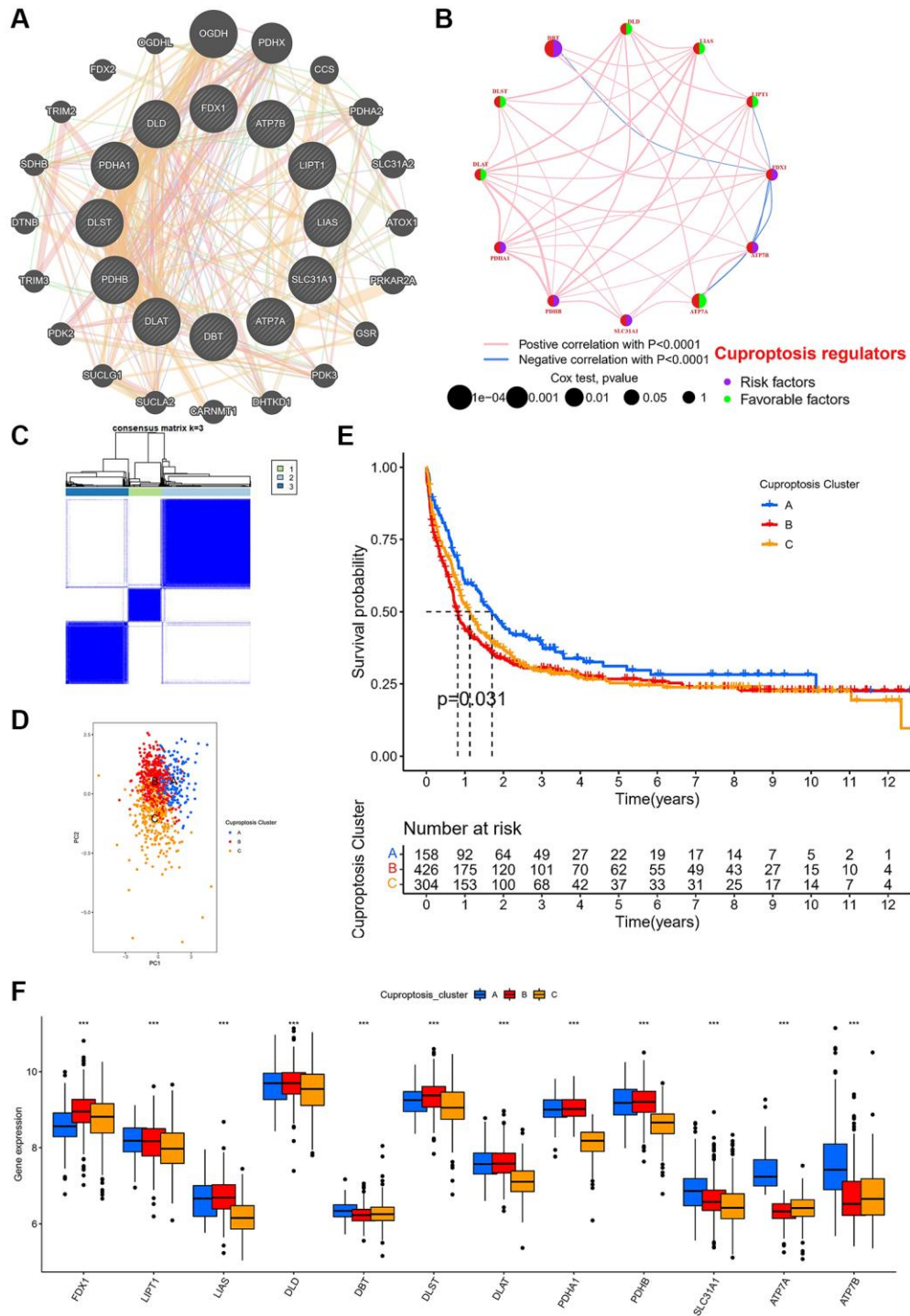

Figure 2. Cuprotosis modification patterns identified with K-means clustering based on cuprotosis genes. (**A**) PPI network showing the interactions of the 12 cuprotosis-related genes. (**B**) The interactions of the 12 cuprotosis-related genes in meta cohort. (**C**) Heat map of unsupervised clustering analysis. (**D**) PCA of different cuprotosis subtypes. (**E**) Kaplan-Meier analysis of overall survival for different cuprotosis subtypes. (**F**) Box plot of cuprotosis-related gene expression in different cuprotosis subtypes in AML patients (*$P < 0.05$, **$P < 0.01$, ***$P < 0.001$).

infiltration of most immune cells, with high expression of activated B cells, CD4$^+$ T cells, CD8$^+$ T cells, dendritic cells, natural killer cells, γδ T cells, neutrophils and type II helper T cells in subtype A (Figure 3A). In addition, the three subtypes of the immune system displayed notable differences in antigen presentation, cytokine receptors, inflammatory response, and T cell activation and suppression (Figure 3B). Additionally, we explored the differences in immune checkpoints among the subtypes and found that there were differences among most immune checkpoints (Figure 3C), with significantly increased expression of
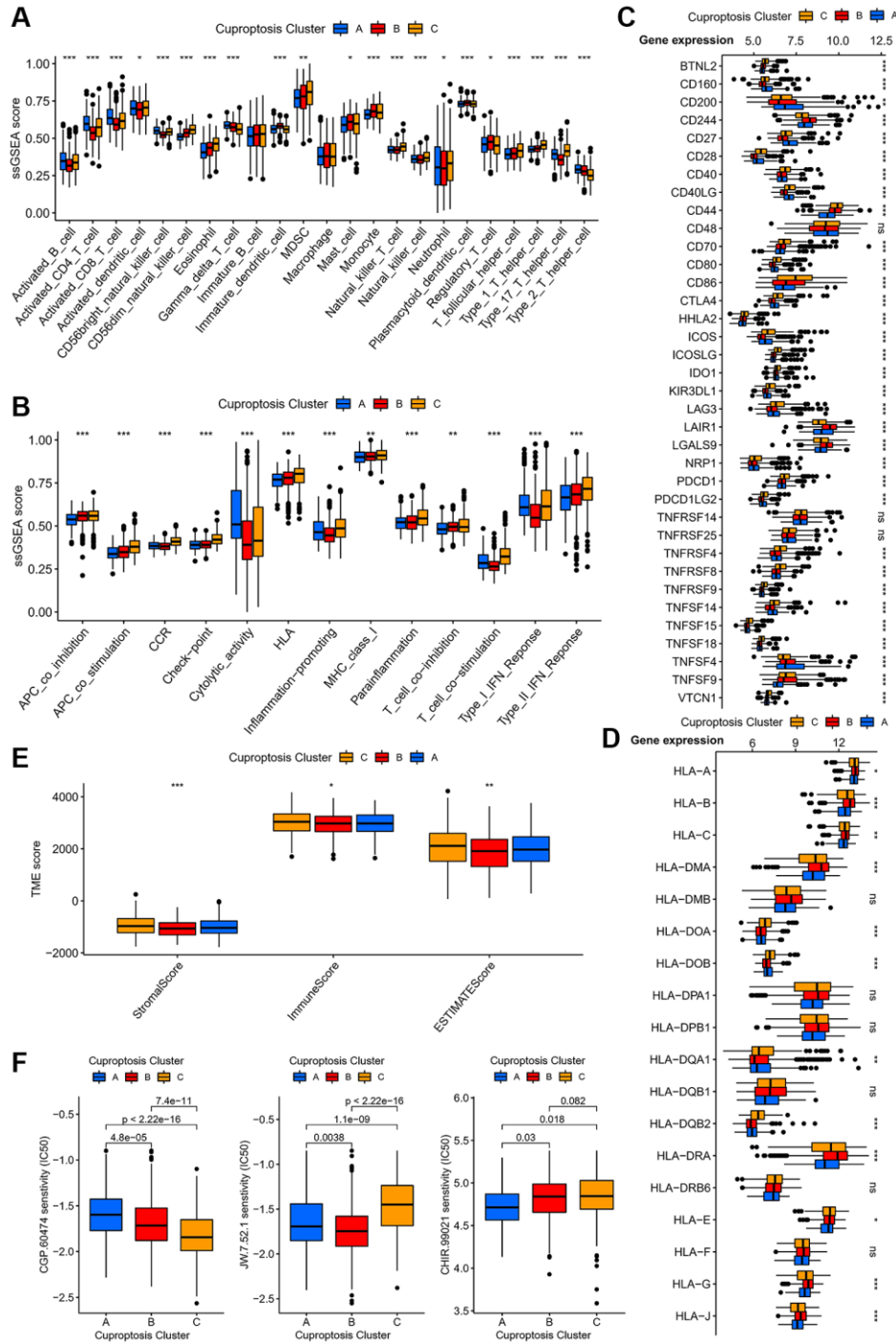

Figure 3. Immunological and biological characteristics of different cuprotosis subtypes. (**A**) Expression of immune-infiltrating cells in different cuprotosis subtypes. (**B**) Relationship between immune cell subsets of different cuprotosis subtypes and immune related functions. (**C**) Expression of immune checkpoints of different cuprotosis subtypes. (**D**) Box plots of the expression of different human leukocyte antigens in the three cuprotosis subtypes. (**E**) Analysis of differences in TME scores for three cuprotosis subtypes. (**F**) IC50 of three targeted drugs in different subtypes. (*$P < 0.05$, **$P < 0.01$, ***$P < 0.001$).

CD160, CD200, and CD27 in subtype A. Importantly, we discovered differences among the subtypes in most human leukocyte antigen class I-related gene (Figure 3D). According to the ESTIMATE algorithm-based results, there were disparities in the tumour micro-environment (TME) scores between the three subtypes, with subtype A score lower on both the immune and stromal scores (Figure 3E). Relevant references have confirmed the important role of the cell cycle, PI3K/mTOR pathway, and Wnt pathway in the progression of AML. It's interesting to note that different subtypes respond differently to specific medications (Figure 3F). Specifically, subtype A was more sensitive to CHIR.99021, subtype B to JW.7.52.1, and subtype C to CGP.60474.

Moreover, we further analyzed the biological functions of different cuprotosis subtypes using GSVA. Enrichment analysis revealed that expression of subtype B was upregulated in the majority of metabolic pathways, including gluconeogenesis, pyruvate metabolism, amino acid metabolism, etc. (Supplementary Figure 3A). Contrarily, subtype A is mainly enriched in the porphyrin and chlorophyll metabolism and cytokinesis pathways (Supplementary Figure 3B), and differences in these pathways may be the reason why subtype A has a higher prognosis for survival when compared to other subtypes. Importantly, almost pathways were enriched in nutrient metabolism and circulation pathways, which was consistent with previous references on the intracellular mechanism of action of CRGs [13].

Characterization and identification of cuprotosis-regulatory subtypes

We identified 525 common DEGs between each other, and the above genes were enriched in cell cycle and metabolic pathways (Supplementary Figure 3C). Similarly, all samples were divided into 2 subtypes by unsupervised cluster analysis performed by DEGs, cuprotosis regulatory subtype A ($n = 492$) and B ($n = 394$) (Supplementary Figure 3D), and survival analysis of the two regulatory subtypes showed that regulatory subtype B had a better median survival time than regulatory subtype A (Supplementary Figure 3E). Subsequently, we analyzed the expression of 12 CRGs in two regulatory subtypes. In detail, the results showed that FDX1, LIAS, DLD, DLAT, PDHA1, PDHB, ATP7A, and ATP7B were significantly different (Supplementary Figure 3F).

Construction and validation of a risk score and prognostic model

The above construction of different subtypes provides some reference value for the prognosis of AML, but the above two kinds of subtypes only represented population. However, the absence of some clinical characteristics and individual assessments may result in clinical practice not being available. We calculated the C-index in all cohorts and selected the LASSO+Cox (stepwise) algorithm as the final model (Figure 4A). In detail, redundant genes were removed by LASSO regression, and 11 regulators were screened and the coefficients of each regulator were calculated by Cox regression (stepwise) analysis (Figure 4B). Next, the AML sample was divided into low-risk and high-risk groups based on risk scores, and patient fatalities increased as risk scores rose (Figure 4C). We further analyzed the expression of 11 regulators in high-risk and low-risk groups of patients in different datasets revealed that the expression of AKR1B1, ID1, SPINT2, and CYB5A was higher in high-risk patients (Figure 5A). Patients in the high-risk category in various data sets all had significantly shorter OS than those in the low-risk group ($p < 0.05$), according to Kaplan-Meier analysis, which was used to examine the impact of different subtypes on prognosis. The AUC value for the TCGA cohort at 1, 3, and 5 years were: 0.634, 0.708 and 0.683, and the AUC value for the GES37642 at 1, 3, and 5 years were: 0.723, 0.760 and 0.751. For GSE12741 cohort, the AUC value at 1 and 3 years were: 0.738 and 0.738 (Figure 5B). In addition, we again performed univariate and multivariate Cox regression analysis on important clinical features (FAB subtype; age; gender; ELN2017 risk category [16]; leukocytes; platelets; bone marrow blasts; runx1-runx1t1 fusion; runx1 mutation) and risk scores to determine whether they were independent prognostic factors for OS, and the results showed that risk score was an independent prognostic factor (Figure 5C).

To predict the cuprotosis model more accurately at the individual level, we first compared the risk scores of different cuprotosis subtypes and cuprotosis regulatory subtypes and found that cuprotosis subtype A and cuprotosis regulatory subtype B had lower risk scores (Supplementary Figure 4A, 4B), which also corresponded to the better prognostic survival described above. Moreover, we used a Sankey diagram to display the association between cuprotosis subtypes, cuprotosis regulatory subtypes, risk score groups, and prognosis. The results revealed that the majority of the subtypes with bad prognoses were significantly linked to high risk and low survival (Supplementary Figure 4C). Finally, we further explored the composition of immune cells, and the results revealed that the high-risk score group exhibited more Tregs cells, fibroblasts, endothelial cells, and other multiple cell infiltrates (Supplementary Figure 4D, 4E).

Validation of the risk score in immunotherapy cohorts

Due to the lack of information on therapeutic agents for AML patients, we selected immunotherapy cohorts (GSE78220 cohort and IMvigor cohort) as validation sets to predict the response to immunotherapy. In the GSE78220 cohort (anti-PD-L1), we discovered that the low-risk score group had a significantly longer median survival time compared to the high-risk group, while in the IMvigor cohort we found that the survival time and response to treatment was better in the high-risk score group than in the low-risk score group after treating PD-1 treatment (Figure 6A, 6B). Overall, our risk score model can, to some extent, guide the treatment of tumors in anti-PD-1 or anti-PD-L1. It's interesting to note that prognostic markers for immunotherapy varied based on the various blocking sites. Finally, we analyzed somatic mutations
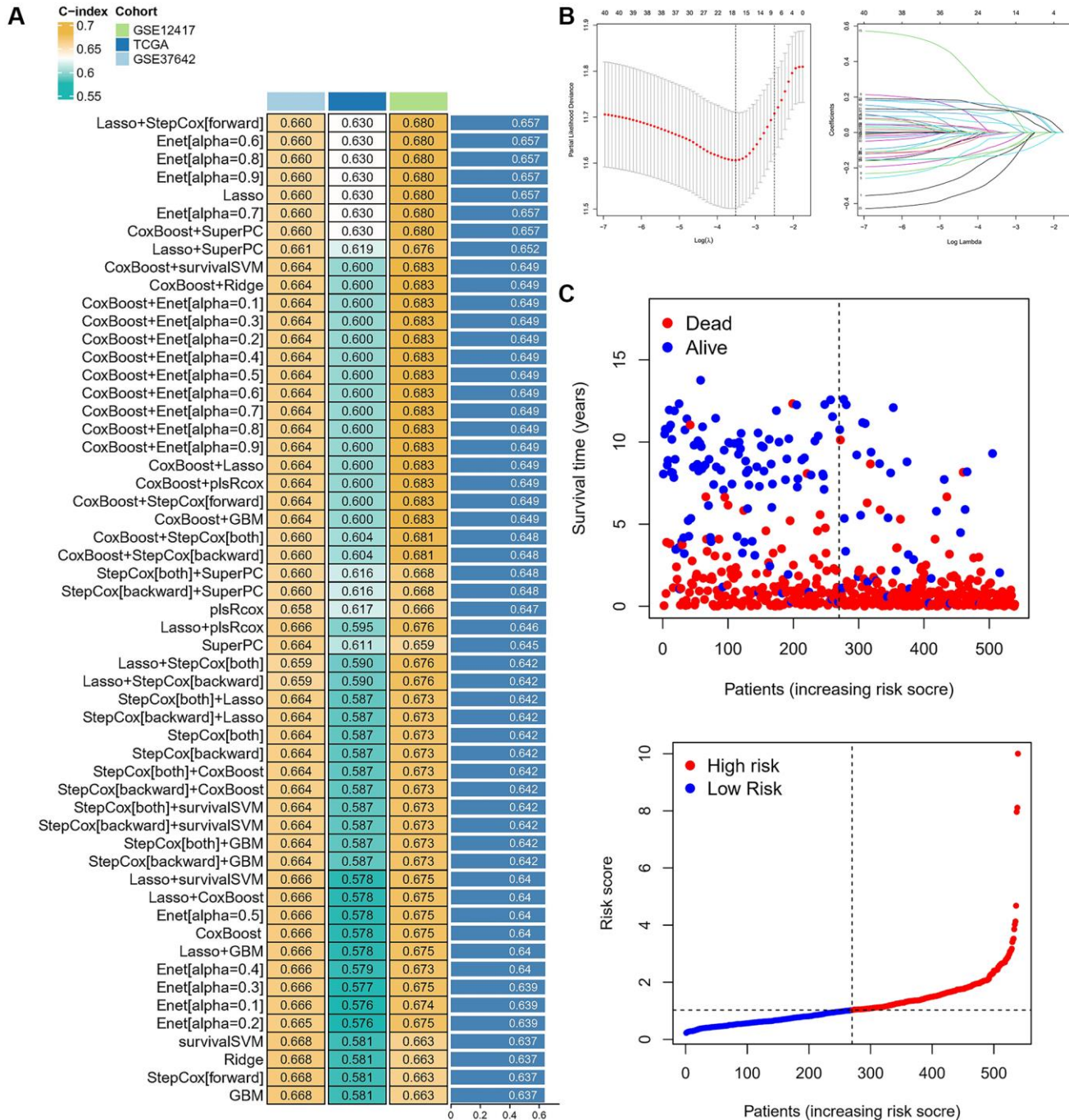

Figure 4. Characterization of different cuprotosis-regulatory subtypes. (**A**) The C-indexes of 55 machine-learning algorithm combinations in the three cohorts. (**B**) LASSO coefficient profiles and cross-validation for tuning the parameter selection in the LASSO analysis. (**C**) Risk Score and Survival Status.

between different risk score subtypes and showed that the frequency of mutations in the KIT gene was higher in the low-risk group, while the frequency of RUNX1 and TP53 mutations was higher in the high-risk group, and these two genes have been included in AML treatment guidelines as molecules with poorer prognosis, but the somatic mutation frequencies were not significantly different between the two groups (Figure 6C, 6D).

Validation of cuprotosis-related genes in peripheral blood

Considering that DBT, DLST, LIPT1 plays a key role in the cuprotosis-related pathways. Hence, we used qRT-PCR to assess three CRGs in blood samples from 12 AML patients and paired normal patients, the average age of the experimental group was 57.67 ± 14.55-years-old,
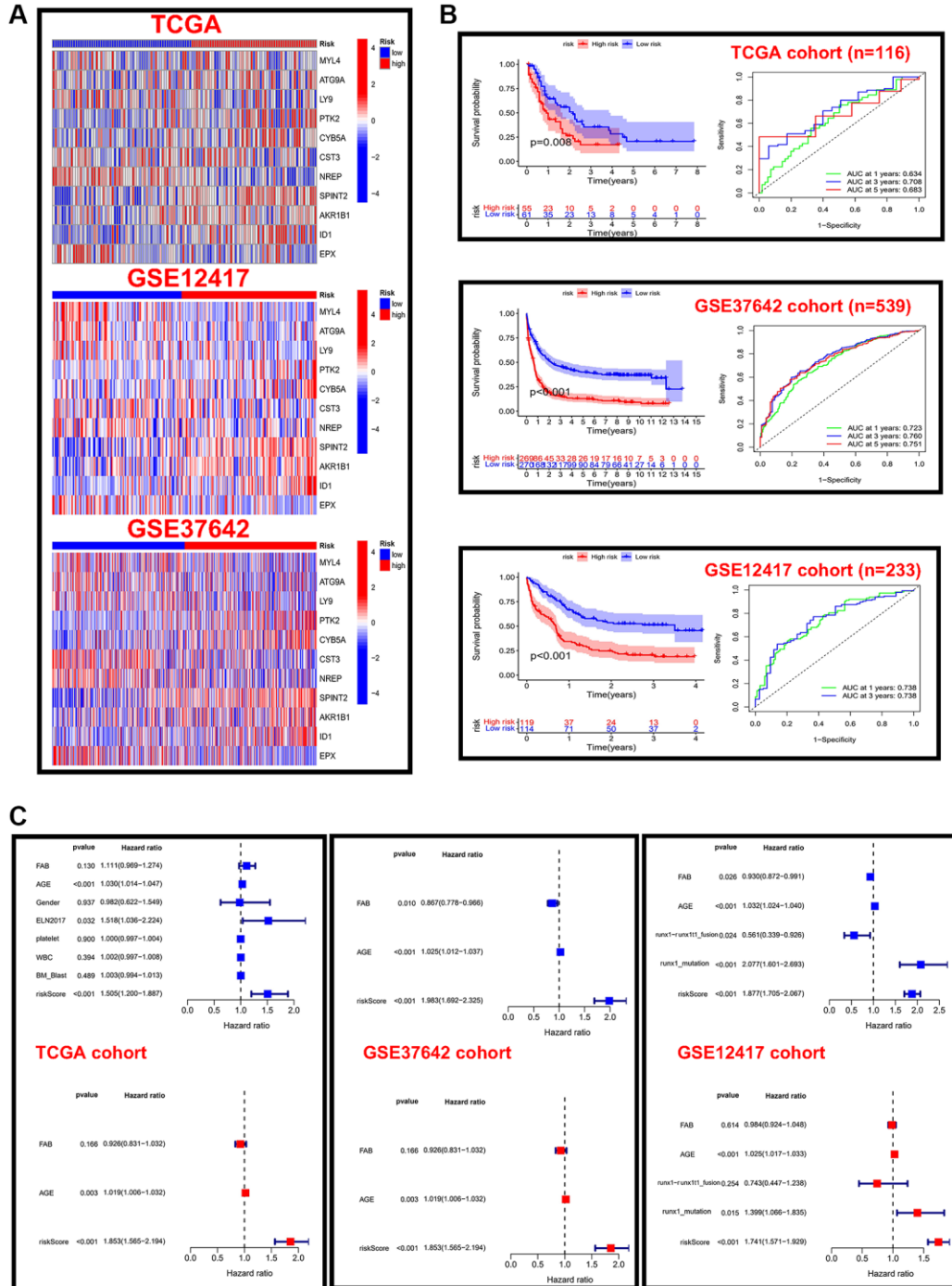

Figure 5. Validation of risk scores in different cohorts. (**A**) Heat map of 11 prognostic model genes expressed in different risk score groups in the TCGA and GEO cohorts. (**B**) Kaplan-Meier analysis and time-dependent ROC curve analysis for different risk score groups in the TCGA cohort. (**C**) Forest plots of independent prognostic factors for univariate and multifactorial Cox analysis in three cohorts.

with a male proportion of 50.00%. The age of the control group was 58.75 ± 10.20-years-old, with a male proportion of 50.00%. There was no statistical difference between the two groups ($P < 0.05$). The results showed that the expression of genes DBT, DLST, LIPT1 was significantly higher in AML patients than in normal patients (Supplementary Figure 5).

Data availability

Publicly available data sets were analyzed in this study. This data can be found here: Publicly available data sets can be obtained from the TCGA (https://portal.gdc.cancer.gov/), GEO (https://www.ncbi.nlm.nih.gov/gds/).
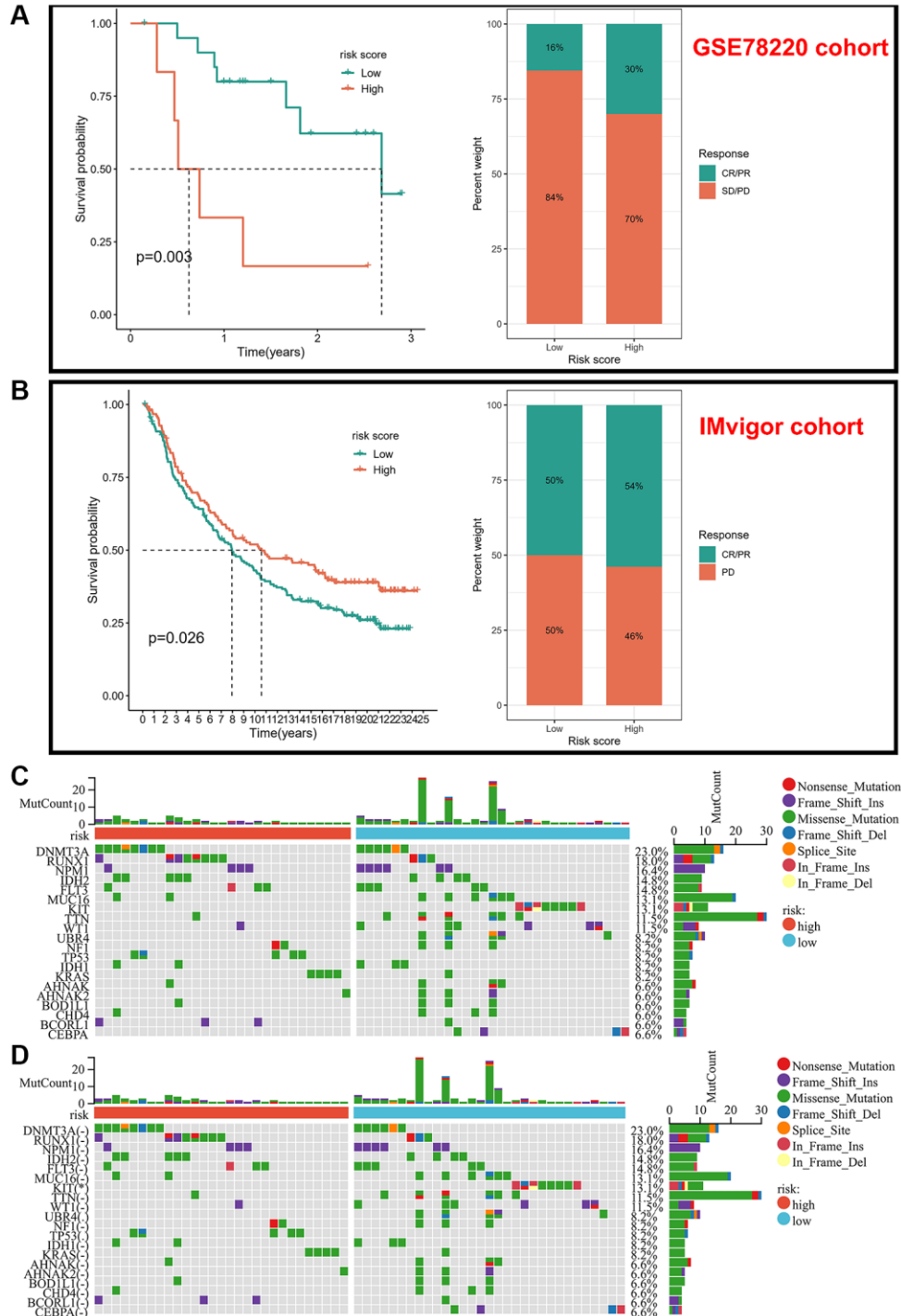

Figure 6. Validation of risk scores in different immunotherapy cohorts. (**A**) Kaplan-Meier analysis of different risk scores and response to drugs in the GSE78220 cohort. (**B**) Kaplan-Meier analysis of different risk scores and response to drugs in the IMvigor-210 cohort. (**C**, **D**) Frequency of somatic mutations in different risk score groups.

Code availability

The code that supports the findings of this study is available from the corresponding author upon request.

DISCUSSION

In recent years, technological advancements in detection, such as next-generation sequencing, have enabled the development of novel and effective treatments for acute myeloid leukemia (AML), including immunotherapy and molecularly targeted drug therapy. However, as one of the common malignant tumors in the blood system [17], despite these advances, AML remains a major challenge for healthcare systems, with its high heterogeneity resulting in low 5-year survival rates, particularly for young patients (35%) [18], and even poorer prognosis for elderly patients aged 65–74 years [19]. Given these challenges, identifying new prognosis-related genes and developing innovative prognostic models are crucial for the stratification of treatment and prognosis of AML patients.

In recent years, the discovery of cuprotosis as a metal-dependent mode of cell death has garnered significant attention in the field of cancer research [10]. This study analyzed the genetic and clinical characteristics of Acute Myeloid Leukemia (AML) patients in the TCGA and GEO datasets, and found that 11 out of the 12 candidate risk genes (CRGs) were differentially expressed between normal patients and AML patients. Further investigation into the prognostic implications of the expression of the 11 genes revealed a correlation between high expression levels of ATP7B, DBT, FDX1, PDHA1, and PDHB and poor prognosis in AML patients. The ATP7B gene, located on human chromosome 13, encodes the production of the copper-transporting P-type ATPase [20]. Elevated expression levels of ATP7B have been shown to negatively impact chemotherapeutic efficacy in various solid tumors [21–24]. FDX1, a mitochondrial metabolic gene, has a crucial role in various processes, including amino acid and sugar metabolism. Abnormal expression of FDX1 can significantly alter cellular behavior, though its specific impact on tumors has yet to be fully understood [25]. The PDHB gene is a key component involved in gluconeogenesis, and previous studies have demonstrated that high expression levels in lung cancer patients are associated with reduced overall survival [26], which is consistent with our findings. The abnormal expression of the other genes analyzed in this study also holds prognostic significance for AML patients.

In our analysis, we classified patients into three distinct cuprotosis subtypes based on the expression levels of the 12 CRGs. Cluster analysis revealed significant differences in the characteristics, biological behavior, TME immune cell infiltration, and patient prognosis among the subtypes. It was observed that the prognosis of subtype A was more favorable compared to the other two subtypes. Further analysis indicated that subtype A exhibited higher cytolytic activity (CYT) and infiltration of multiple immune cells, including activated B cells, CD4+ T cells, CD8+ T cells, and natural killer cells. CYT serves as a measure of inflammation and previous studies have shown that high CYT levels in tumors are associated with better overall survival rates [27]. Another study has previously suggested that immune cells CYT could serve as an indicator for the efficacy of immune checkpoint inhibitor therapy in prostate cancer patients. Furthermore, this study determined a correlation between immune cell CYT and overall immune function, with a notable increase in the proportion of CD8+ T cells in the group with high CYT expression as compared to the group with low CYT expression [28]. This result aligns with our findings.

We employed a comprehensive analysis, utilizing 55 combinations of machine learning algorithms to build models in various datasets, and differentiated high-risk and low-risk subtypes based on the results of these models. Our findings indicate that there are significant differences between the two subtypes, which were validated in multiple cohorts, including cuprotosis subtypes and cuprotosis regulatory subtypes, and in certain solid tumors. The lower risk scores for both cuprotosis subtype A and cuprotosis regulatory subtype B may also account for the better prognosis in these two groups. In addition, after incorporating more important clinical characteristics, univariate and multifactor COX regression analyses still showed that our risk score model could be used as an independent factor for prognosis, fully illustrating the stability of the model. Additionally, our analysis of the biological behavior of the different risk subtypes revealed that the high-risk score group exhibited higher infiltration of Tregs cells, endothelial cells, and macrophages. This observation may be associated with a poor prognosis. As a type of immunosuppressive cells, high expression of Tregs cells has been shown to result in the escape of tumor cells [29, 30]. Studies have reported that the expression of Tregs cells is higher in acute myeloid leukemia (AML) patients compared to healthy individuals [31], and that Tregs contribute to immune escape through the suppression of anti-leukemia treatment [32]. Macrophages, as a component of immune cells, play a crucial role in the inflammatory and tumor microenvironment [33], and are often implicated in the establishment of a microenvironment that is favorable to tumor progression through various mechanisms [34]. Tumor-

associated macrophages promote tumorigenesis and progression by expressing pro-inflammatory cytokines in an inappropriate manner through disrupted inflammatory signaling pathways [35], and this inflammatory state also contributes to the progression of chronic lymphocytic leukemia (CLL) and the extramedullary infiltration of T acute lymphocytic leukemia (T-ALL) [36, 37]. Importantly, immunotherapy is a widely researched area in cancer treatment and is gaining prominence for improving the cure rate and long-term survival of patients. This includes therapies such as PD-1 antibody and chimeric antigen receptor T cell therapy [38–41]. Our risk score model demonstrated significant differences across the groups receiving PD-1 or PD-L1 therapy, implying that our model holds potential in guiding the application of immunotherapy.

There are some limitations to our research. We only utilized public databases for initial exploration and did not examine real-world data, there may be differences in geography, skin color, age, and other aspects. Additionally, we lack sufficient information about immunotherapy for AML patients, which will be the focus of our future efforts.

In conclusion, as a preliminary study of cuprotosis in AML, we demonstrated the relationship between cuprotosis-related genes, cuprotosis subtypes and prognosis of AML patients. Our study well demonstrates the prognostic value of cuprotosis in AML patients and will inform new AML therapeutic targets.

Abbreviations

AML: Acute myeloid leukemia; CLL: chronic lymphocytic leukemia; CRGs: cuprotosis-related genes; DEGs: differentially expressed genes; TME: tumor microenvironment; PCA: principal component analysis; TCGA: The Cancer Genome Atlas; CNV: copy number variation; GEO: Gene Expression Omnibus; GSVA: gene set variation analysis; ssGSEA: single sample gene set enrichment analysis; LASSO: least absolute shrinkage and selection operator; T-ALL: T acute lymphocytic leukemia; CYT: cytolytic activity.

AUTHOR CONTRIBUTIONS

All authors participated in the study, Yanhui Wei and Songwei Feng conceived and designed the study, Yanhui Wei wrote the first draft of the manuscript, Songwei Feng participated in the statistics and analysis of the paper, Zhaoxu Miao mainly participated in the collection and preliminary processing of samples, and Xuejun Guo participated in the supervision of the article and the collection of clinical data and experiments,

Songwei Feng and Xuejun Guo jointly reviewed the manuscript.

CONFLICTS OF INTEREST

The authors declare no conflicts of interest related to this study.

ETHICAL STATEMENT AND CONSENT

Approval was obtained from the ethics committee of Puyang Oilfield General Hospital Affiliated with Xinxiang Medical University. The procedures used in this study adhere to the tenets of the Declaration of Helsinki. All clinical samples utilized in this study obtained with written consent from the respective patients.

Editorial note

&This corresponding author has a verified history of publications using a personal email address for correspondence.

REFERENCES

1. Shi X, Jiang Y, Kitano A, Hu T, Murdaugh RL, Li Y, Hoegenauer KA, Chen R, Takahashi K, Nakada D. Nuclear NAD+ homeostasis governed by NMNAT1 prevents apoptosis of acute myeloid leukemia stem cells. Sci Adv. 2021; 7:eabf3895.
https://doi.org/10.1126/sciadv.abf3895
PMID:34290089

2. Genovese G, Kähler AK, Handsaker RE, Lindberg J, Rose SA, Bakhoum SF, Chambert K, Mick E, Neale BM, Fromer M, Purcell SM, Svantesson O, Landén M, et al. Clonal Hematopoiesis and Blood-Cancer Risk Inferred from Blood DNA Sequence. N Engl J Med. 2014; 371: 2477–87.
https://doi.org/10.1056/NEJMoa1409405

3. Shimony S, Stahl M, Stone RM. Acute myeloid leukemia: 2023 update on diagnosis, risk-stratification, and management. Am J Hematol. 2023; 98:502–26.
https://doi.org/10.1002/ajh.26822
PMID:36594187

4. Takahashi K, Wang F, Kantarjian H, Doss D, Khanna K, Thompson E, Zhao L, Patel K, Neelapu S, Gumbs C, Bueso-Ramos C, DiNardo CD, Colla S, et al. Preleukaemic clonal haemopoiesis and risk of therapy-related myeloid neoplasms: a case-control study. Lancet Oncol. 2017; 18:100–11.
https://doi.org/10.1016/S1470-2045(16)30626-X
PMID:27923552

5. Padmakumar D, Chandraprabha VR, Gopinath P,

Vimala Devi ART, Anitha GRJ, Sreelatha MM, Padmakumar A, Sreedharan H. A concise review on the molecular genetics of acute myeloid leukemia. Leuk Res. 2021; 111:106727.
https://doi.org/10.1016/j.leukres.2021.106727
PMID:34700049

6. Itzykson R, Fournier E, Berthon C, Röllig C, Braun T, Marceau-Renaut A, Pautas C, Nibourel O, Lemasle E, Micol JB, Adès L, Lebon D, Malfuson JV, et al. Genetic identification of patients with AML older than 60 years achieving long-term survival with intensive chemotherapy. Blood. 2021; 138:507–19.
https://doi.org/10.1182/blood.2021011103
PMID:34410352

7. Zeng AGX, Bansal S, Jin L, Mitchell A, Chen WC, Abbas HA, Chan-Seng-Yue M, Voisin V, van Galen P, Tierens A, Cheok M, Preudhomme C, Dombret H, et al. A cellular hierarchy framework for understanding heterogeneity and predicting drug response in acute myeloid leukemia. Nat Med. 2022; 28:1212–23.
https://doi.org/10.1038/s41591-022-01819-x
PMID:35618837

8. Jiang X, Stockwell BR, Conrad M. Ferroptosis: mechanisms, biology and role in disease. Nat Rev Mol Cell Biol. 2021; 22:266–82.
https://doi.org/10.1038/s41580-020-00324-8
PMID:33495651

9. Ketelut-Carneiro N, Fitzgerald KA. Apoptosis, Pyroptosis, and Necroptosis-Oh My! The Many Ways a Cell Can Die. J Mol Biol. 2022; 434:167378.
https://doi.org/10.1016/j.jmb.2021.167378
PMID:34838807

10. Tsvetkov P, Coy S, Petrova B, Dreishpoon M, Verma A, Abdusamad M, Rossen J, Joesch-Cohen L, Humeidi R, Spangler RD, Eaton JK, Frenkel E, Kocak M, et al. Copper induces cell death by targeting lipoylated TCA cycle proteins. Science. 2022; 375:1254–61.
https://doi.org/10.1126/science.abf0529
PMID:35298263

11. Lutsenko S. Dynamic and cell-specific transport networks for intracellular copper ions. J Cell Sci. 2021; 134:jcs240523.
https://doi.org/10.1242/jcs.240523
PMID:34734631

12. Xue Q, Kang R, Klionsky DJ, Tang D, Liu J, Chen X. Copper metabolism in cell death and autophagy. Autophagy. 2023; 1–21. [Epub ahead of print].
https://doi.org/10.1080/15548627.2023.2200554
PMID:37055935

13. Li SR, Bu LL, Cai L. Cuproptosis: lipoylated TCA cycle proteins-mediated novel cell death pathway. Signal Transduct Target Ther. 2022; 7:158.
https://doi.org/10.1038/s41392-022-01014-x
PMID:35562341

14. Ge EJ, Bush AI, Casini A, Cobine PA, Cross JR, DeNicola GM, Dou QP, Franz KJ, Gohil VM, Gupta S, Kaler SG, Lutsenko S, Mittal V, et al. Connecting copper and cancer: from transition metal signalling to metalloplasia. Nat Rev Cancer. 2022; 22:102–13.
https://doi.org/10.1038/s41568-021-00417-2
PMID:34764459

15. Liu Z, Liu L, Weng S, Guo C, Dang Q, Xu H, Wang L, Lu T, Zhang Y, Sun Z, Han X. Machine learning-based integration develops an immune-derived lncRNA signature for improving outcomes in colorectal cancer. Nat Commun. 2022; 13:816.
https://doi.org/10.1038/s41467-022-28421-6
PMID:35145098

16. Döhner H, Estey E, Grimwade D, Amadori S, Appelbaum FR, Büchner T, Dombret H, Ebert BL, Fenaux P, Larson RA, Levine RL, Lo-Coco F, Naoe T, et al. Diagnosis and management of AML in adults: 2017 ELN recommendations from an international expert panel. Blood. 2017; 129:424–47.
https://doi.org/10.1182/blood-2016-08-733196
PMID:27895058

17. Newell LF, Cook RJ. Advances in acute myeloid leukemia. BMJ. 2021; 375:n2026.
https://doi.org/10.1136/bmj.n2026
PMID:34615640

18. Daver N, Wei AH, Pollyea DA, Fathi AT, Vyas P, DiNardo CD. New directions for emerging therapies in acute myeloid leukemia: the next chapter. Blood Cancer J. 2020; 10:107.
https://doi.org/10.1038/s41408-020-00376-1
PMID:33127875

19. Sorror ML, Storer BE, Fathi AT, Brunner A, Gerds AT, Sekeres MA, Mukherjee S, Medeiros BC, Wang ES, Vachhani P, Shami PJ, Peña E, Elsawy M, et al. Multisite 11-year experience of less-intensive vs intensive therapies in acute myeloid leukemia. Blood. 2021; 138:387–400.
https://doi.org/10.1182/blood.2020008812
PMID:34351368

20. Zhou X, Zhou W, Wang C, Wang L, Jin Y, Jia Z, Liu Z, Zheng B. A Comprehensive Analysis and Splicing Characterization of Naturally Occurring Synonymous Variants in the ATP7B Gene. Front Genet. 2020; 11:592611.
https://doi.org/10.3389/fgene.2020.592611
PMID:33719328

21. Lukanović D, Herzog M, Kobal B, Černe K. The contribution of copper efflux transporters ATP7A and

ATP7B to chemoresistance and personalized medicine in ovarian cancer. Biomed Pharmacother. 2020; 129:110401.
https://doi.org/10.1016/j.biopha.2020.110401
PMID:32570116

22. Shanbhag V, Jasmer-McDonald K, Zhu S, Martin AL, Gudekar N, Khan A, Ladomersky E, Singh K, Weisman GA, Petris MJ. ATP7A delivers copper to the lysyl oxidase family of enzymes and promotes tumorigenesis and metastasis. Proc Natl Acad Sci U S A. 2019; 116:6836–41.
https://doi.org/10.1073/pnas.1817473116
PMID:30890638

23. Nakagawa T, Inoue Y, Kodama H, Yamazaki H, Kawai K, Suemizu H, Masuda R, Iwazaki M, Yamada S, Ueyama Y, Inoue H, Nakamura M. Expression of copper-transporting P-type adenosine triphosphatase (ATP7B) correlates with cisplatin resistance in human non-small cell lung cancer xenografts. Oncol Rep. 2008; 20:265–70.
PMID:18636185

24. Yu Z, Cao W, Ren Y, Zhang Q, Liu J. ATPase copper transporter A, negatively regulated by miR-148a-3p, contributes to cisplatin resistance in breast cancer cells. Clin Transl Med. 2020; 10:57–73.
https://doi.org/10.1002/ctm2.19
PMID:32508020

25. Zhang Z, Ma Y, Guo X, Du Y, Zhu Q, Wang X, Duan C. FDX1 can Impact the Prognosis and Mediate the Metabolism of Lung Adenocarcinoma. Front Pharmacol. 2021; 12:749134.
https://doi.org/10.3389/fphar.2021.749134
PMID:34690780

26. Giannos P, Kechagias KS, Gal A. Identification of Prognostic Gene Biomarkers in Non-Small Cell Lung Cancer Progression by Integrated Bioinformatics Analysis. Biology (Basel). 2021; 10:1200.
https://doi.org/10.3390/biology10111200
PMID:34827193

27. Fujita M, Yamaguchi R, Hasegawa T, Shimada S, Arihiro K, Hayashi S, Maejima K, Nakano K, Fujimoto A, Ono A, Aikata H, Ueno M, Hayami S, et al. Classification of primary liver cancer with immunosuppression mechanisms and correlation with genomic alterations. EBioMedicine. 2020; 53:102659.
https://doi.org/10.1016/j.ebiom.2020.102659
PMID:32113157

28. Gao Z, Tao Y, Lai Y, Wang Q, Li Z, Peng S, Chen J, Cai W, Li K, Huang H. Immune Cytolytic Activity as an Indicator of Immune Checkpoint Inhibitors Treatment for Prostate Cancer. Front Bioeng Biotechnol. 2020; 8:930.
https://doi.org/10.3389/fbioe.2020.00930

PMID:32850758

29. Tanaka A, Sakaguchi S. Targeting Treg cells in cancer immunotherapy. Eur J Immunol. 2019; 49:1140–6.
https://doi.org/10.1002/eji.201847659
PMID:31257581

30. Lee GR. Phenotypic and Functional Properties of Tumor-Infiltrating Regulatory T Cells. Mediators Inflamm. 2017; 2017:5458178.
https://doi.org/10.1155/2017/5458178
PMID:29463952

31. Wang M, Zhang C, Tian T, Zhang T, Wang R, Han F, Zhong C, Hua M, Ma D. Increased Regulatory T Cells in Peripheral Blood of Acute Myeloid Leukemia Patients Rely on Tumor Necrosis Factor (TNF)-α-TNF Receptor-2 Pathway. Front Immunol. 2018; 9:1274.
https://doi.org/10.3389/fimmu.2018.01274
PMID:29922294

32. Delia M, Carluccio P, Mestice A, Frappampina R, Albano F, Specchia G, Musto P. After Treatment Decrease of Bone Marrow Tregs and Outcome in Younger Patients with Newly Diagnosed Acute Myeloid Leukemia. J Immunol Res. 2020; 2020:2134647.
https://doi.org/10.1155/2020/2134647
PMID:33204734

33. Rath M, Müller I, Kropf P, Closs EI, Munder M. Metabolism via Arginase or Nitric Oxide Synthase: Two Competing Arginine Pathways in Macrophages. Front Immunol. 2014; 5:532.
https://doi.org/10.3389/fimmu.2014.00532
PMID:25386178

34. Wang D, Yang L, Yue D, Cao L, Li L, Wang D, Ping Y, Shen Z, Zheng Y, Wang L, Zhang Y. Macrophage-derived CCL22 promotes an immunosuppressive tumor microenvironment via IL-8 in malignant pleural effusion. Cancer Lett. 2019; 452:244–53.
https://doi.org/10.1016/j.canlet.2019.03.040
PMID:30928379

35. Szebeni GJ, Vizler C, Kitajka K, Puskas LG. Inflammation and Cancer: Extra- and Intracellular Determinants of Tumor-Associated Macrophages as Tumor Promoters. Mediators Inflamm. 2017; 2017:9294018.
https://doi.org/10.1155/2017/9294018
PMID:28197019

36. Schulz A, Toedt G, Zenz T, Stilgenbauer S, Lichter P, Seiffert M. Inflammatory cytokines and signaling pathways are associated with survival of primary chronic lymphocytic leukemia cells in vitro: a dominant role of CCL2. Haematologica. 2011; 96:408–16.
https://doi.org/10.3324/haematol.2010.031377

PMID:21134984

37. Yang F, Feng W, Wang H, Wang L, Liu X, Wang R, Chen C, Yang X, Zhang D, Ren Q, Zheng G. Monocyte-Derived Leukemia-Associated Macrophages Facilitate Extramedullary Distribution of T-cell Acute Lymphoblastic Leukemia Cells. Cancer Res. 2020; 80:3677–91.
https://doi.org/10.1158/0008-5472.CAN-20-0034
PMID:32651260

38. Xu-Monette ZY, Zhou J, Young KH. PD-1 expression and clinical PD-1 blockade in B-cell lymphomas. Blood. 2018; 131:68–83.
https://doi.org/10.1182/blood-2017-07-740993
PMID:29118007

39. Long J, Lin J, Wang A, Wu L, Zheng Y, Yang X, Wan X, Xu H, Chen S, Zhao H. PD-1/PD-L blockade in gastrointestinal cancers: lessons learned and the road toward precision immunotherapy. J Hematol Oncol. 2017; 10:146.
https://doi.org/10.1186/s13045-017-0511-2
PMID:28774337

40. Dai X, Gao Y, Wei W. Post-translational regulations of PD-L1 and PD-1: Mechanisms and opportunities for combined immunotherapy. Semin Cancer Biol. 2022; 85:246–52.
https://doi.org/10.1016/j.semcancer.2021.04.002
PMID:33831533

41. Singh AK, McGuirk JP. CAR T cells: continuation in a revolution of immunotherapy. Lancet Oncol. 2020; 21:e168–78.
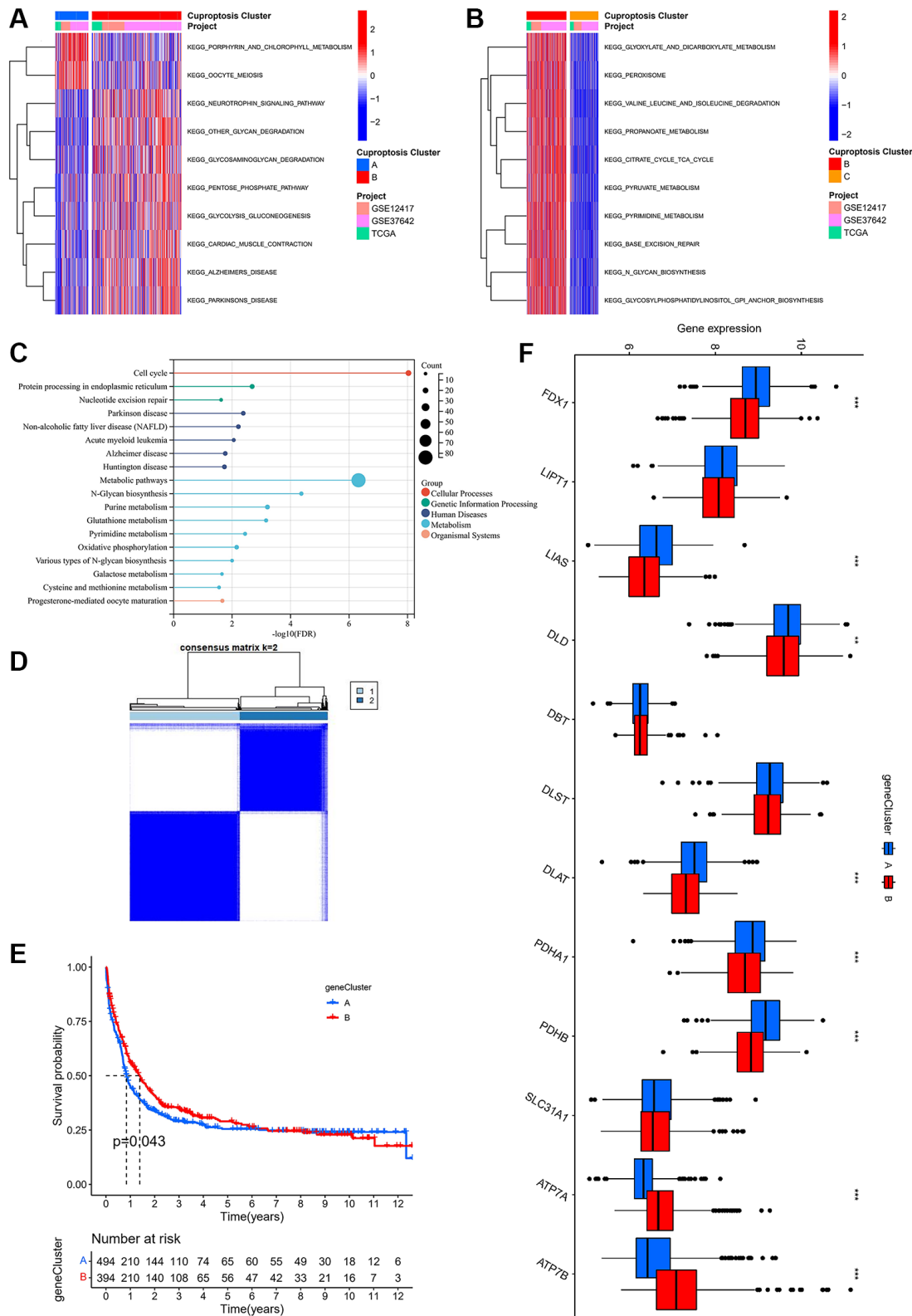https://doi.org/10.1016/S1470-2045(19)30823-X
PMID:32135120
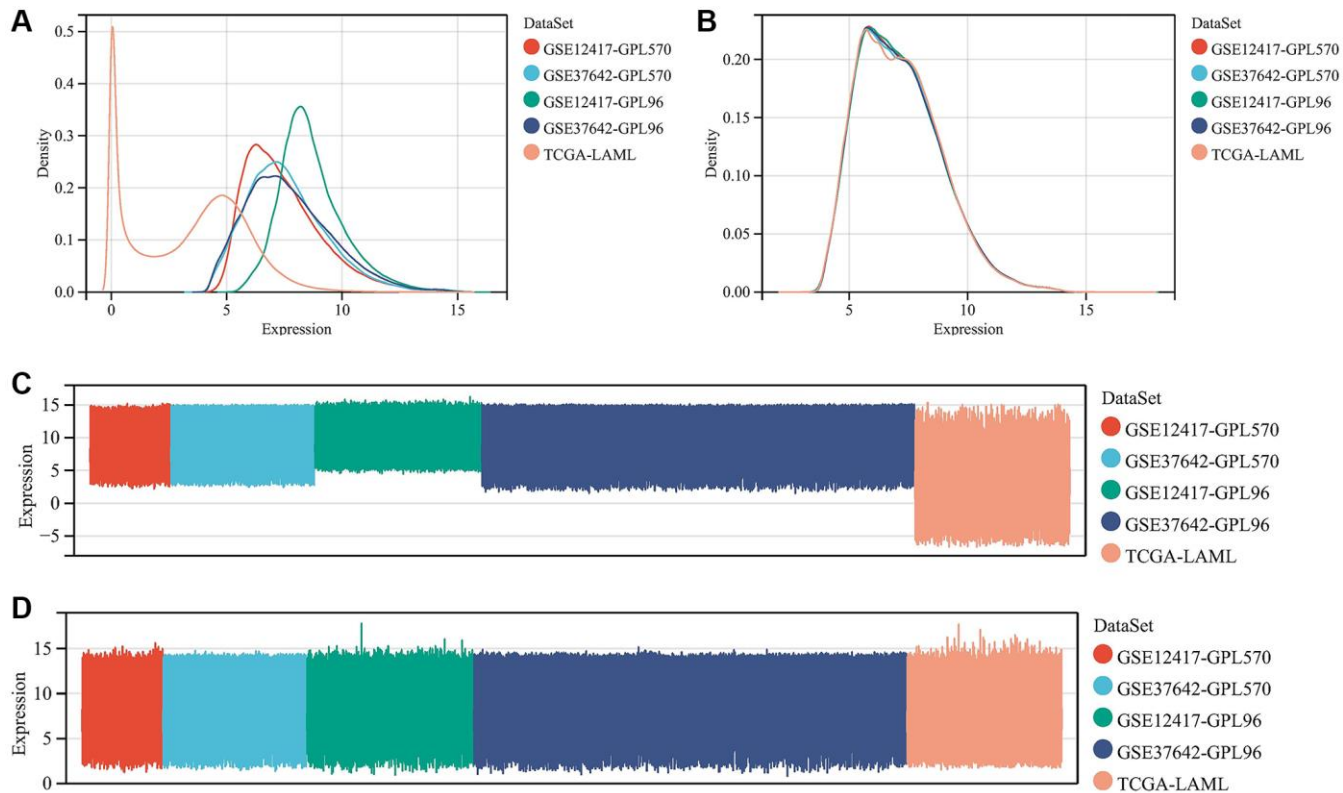
Supplementary Figure 1. Normalization of multiple cohorts. (**A**, **C**) Data characteristics before normalization of the five cohorts. (**B**, **D**) Data characteristics after normalization of the five cohorts.
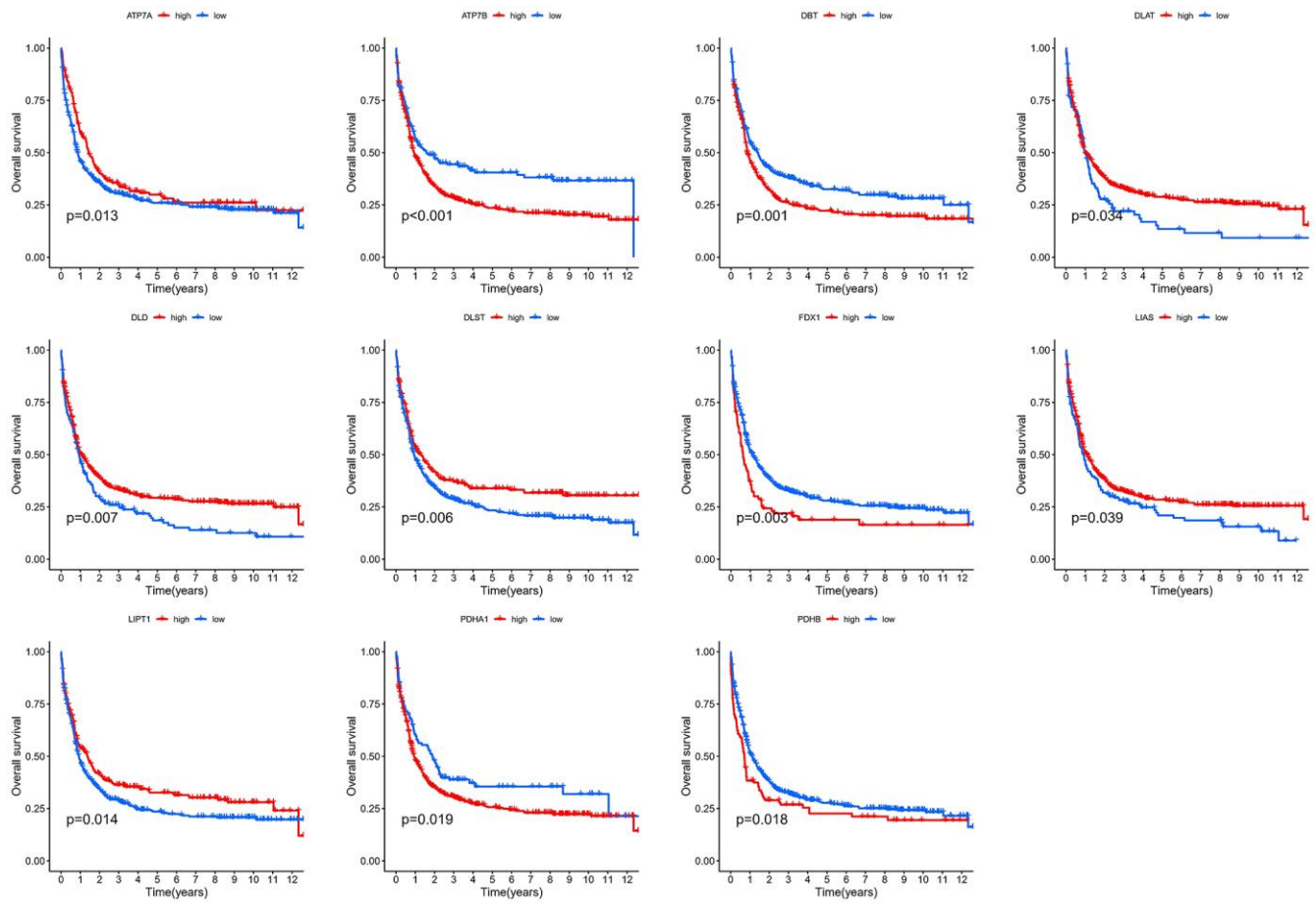
Supplementary Figure 2. Kaplan-Meier analysis of 11 cuprotosis-related genes.

Supplementary Figure 3. Characterization of different cuprotosis-regulatory subtypes. (**A**) Heat map showing KEGG enrichment analysis of cuprotosis subtypes **A** and **B**. (**B**) Heat map showing KEGG enrichment analysis of cuprotosis subtypes **B** and **C**. (**C**) Functional enrichment analysis of DEGs. (**D**) Heat map of unsupervised clustering analysis. (**E**) Kaplan-Meier analysis of overall survival curves for different cuprotosis-regulatory subtypes. (**F**) Box plot of cuprotosis-related genes expression in different cuprotosis-regulatory subtypes ($^*P < 0.05$, $^{**}P < 0.01$, $^{***}P < 0.001$).
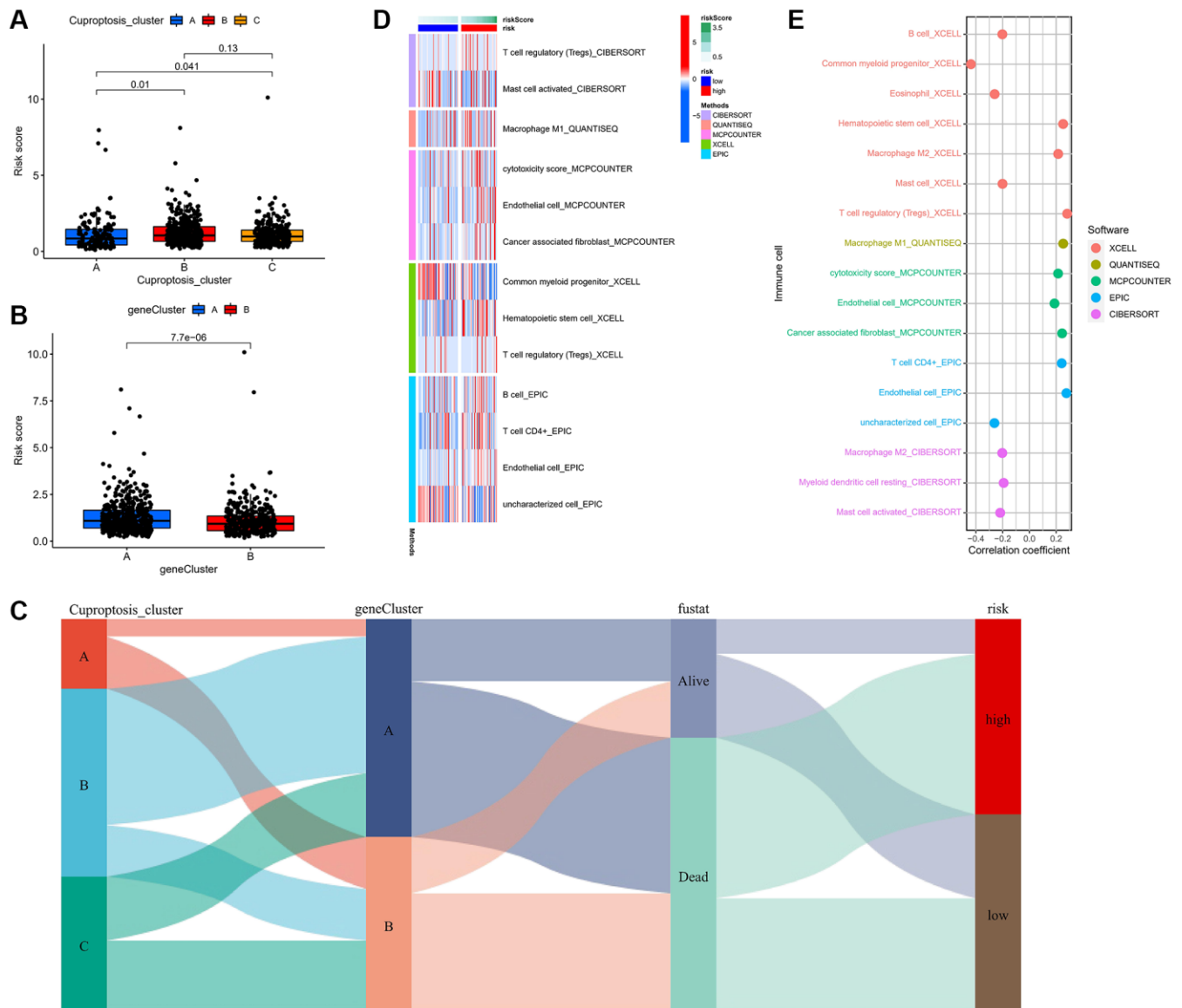
Supplementary Figure 4. TME characteristics of risk score and their relevance with molecular subtypes. (**A**) Risk scores for different cuprotosis subtypes. (**B**) Risk scores for different cuprotosis-regulatory subtypes. (**C**) The relevance in cuprotosis subtypes, cuprotosis-regulatory subtypes, risk score, and survival status. (**D**) Heat map showing the relationship between different risk score groups and immune cells. (**E**) Bubble plots showing the relationship between different risk score groups and immune cells.
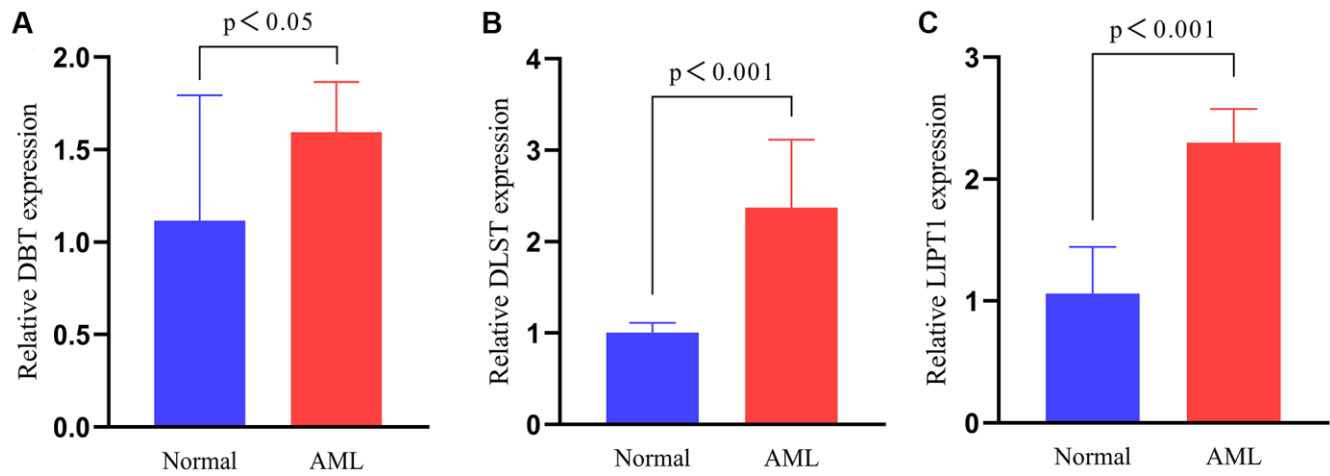
Supplementary Figure 5. Expression of three cuprotosis-related genes in clinical samples. (**A**) Expression of DBT gene in normal human and AML patients. (**B**) Expression of DLST gene in normal human and AML patients. (**C**) Expression of LIPT1 gene in normal human and AML patients.